

UNIMODULAR SEQUENCE DESIGN FOR GOOD AUTOCORRELATION PROPERTIES

Hao He[†], Petre Stoica[‡] and Jian Li[†]

[†]Dept. of Electrical and Computer Engineering, University of Florida, Gainesville, FL, USA

[‡] Dept. of Information Technology, Uppsala University, Uppsala, Sweden

ABSTRACT

Unimodular (i.e., constant modulus) sequences with good autocorrelation properties are useful in several areas, including communications, radar and sonar. The integrated sidelobe level (ISL) is often used to express the goodness of the autocorrelation properties of a given sequence. In this paper, we present several cyclic algorithms for the local minimization of ISL-related metrics. To illustrate the performance of the proposed algorithms, we present a number of examples including the design of sequences that have virtually zero autocorrelation sidelobes in a specified lag interval, and of long sequences that could hardly be handled by means of other algorithms previously suggested in the literature.

Index Terms— Waveform design, unimodular sequences, integrated sidelobe level, merit factor, autocorrelation.

1. INTRODUCTION & PROBLEM FORMULATION

Let $\{x_n\}_{n=1}^N$ denote the sequence to be designed with the unimodular constraint $|x_n| = 1$, $n = 1, \dots, N$ and let

$$r_k = \sum_{n=k+1}^N x_n x_{n-k}^* = r_{-k}^*, \quad k = 0, \dots, N-1 \quad (1)$$

be the autocorrelation function of $\{x_n\}_{n=1}^N$, where $(\cdot)^*$ denotes the complex conjugate for scalars and the conjugate transpose for vectors and matrices. The goodness of the autocorrelation properties of $\{x_n\}_{n=1}^N$ is often expressed by a small integrated sidelobe level (ISL) or a large merit factor (MF), which are defined as

$$\text{ISL} = \sum_{k=1}^{N-1} |r_k|^2 \quad \text{and} \quad \text{MF} = \frac{|r_0|^2}{2 \text{ISL}} = \frac{N^2}{2 \text{ISL}}, \quad (2)$$

respectively. Unimodular sequences with large MF values are desired in many applications, including wireless communications and range compression radar and sonar. In these applications, an emitted (probing or training) sequence with a large

This work was supported in part by the Office of Naval Research (ONR) under Grants No. N00014-07-1-0193 and N00014-07-1-0293, the Army Research Office (ARO) under Grant No. W911NF-07-1-0450, the National Science Foundation (NSF) under Grant No. CCF-0634786, the Swedish Research Council (VR) and the European Research Council (ERC). Opinions, interpretations, conclusions, and recommendations are those of the authors and are not necessarily endorsed by the United States Government.

MF reduces the risk that the received sequence of interest is drawn in correlated multipath or clutter interferences. Additionally, the limitations of the sequence generation hardware lead to the requirement that the emitted sequence be unimodular. Owing to the significant theoretical and practical interest, the literature is extensive on the design of unimodular sequences with good correlation properties (hereafter, correlation exclusively means autocorrelation), see [1]–[14] and the many references therein. Because the ISL metric may be highly multimodal (i.e., it may have multiple local minima), stochastic optimization algorithms have been suggested for its minimization (see, e.g., [3][6][7]). However, these algorithms are computationally expensive and usually are only effective for $N \sim 10^2$.

In this paper, we introduce several cyclic algorithms (CA, see [12][13][14]) for the local minimization of ISL-related metrics, namely CA-pruned (CAP), CA-new (CAN) and weighted-CAN (WeCAN). CAN locally minimizes the ISL metric in Eq. (2) and can be used to design very long sequences, up to $N \sim 10^6$ or even larger. CAP and WeCAN deal with weighted correlation metrics of the form

$$\text{WISL} = \sum_{k=1}^{N-1} w_k |r_k|^2, \quad \text{MMF} = \frac{|r_0|^2}{2 \text{WISL}} = \frac{N^2}{2 \text{WISL}}$$

$$w_k \geq 0, \quad k = 1, \dots, N-1 \quad (3)$$

and they can be used for sequence lengths $N \sim 10^3$.

2. CAP

CAP (CA-pruned) is an extension of the CA in [14]. Define

$$\bar{\mathbf{X}} = \begin{bmatrix} x_1 & & & 0 \\ \vdots & \ddots & & \\ \vdots & & x_1 & \\ x_N & & \vdots & \\ 0 & & \ddots & \vdots \\ & & & x_N \end{bmatrix}_{(N+P-1) \times P}, \quad \tilde{\mathbf{X}}_{(N+P-1) \times Q} = \bar{\mathbf{X}} \mathbf{T}, \quad (4)$$

where the $P \times Q$ ($Q \leq P \leq N$) matrix \mathbf{T} is made from Q selected columns of the $P \times P$ identity matrix \mathbf{I}_P . For example, if we are interested in suppressing $r_{k_1}, \dots, r_{k_{Q-1}}$,

we should select the first column, the $(k_1 + 1)^{\text{th}}$ column, ..., up to the $(k_{Q-1} + 1)^{\text{th}}$ column of \mathbf{I}_P to construct the \mathbf{T} in Eq. (4). A simple situation is to suppress r_1, \dots, r_{P-1} , in which case we should choose $Q = P$, which leads to $\tilde{\mathbf{X}} = \tilde{\mathbf{X}}$ and

$$\tilde{\mathbf{X}}^* \tilde{\mathbf{X}} = \begin{bmatrix} r_0 & r_1^* & \cdots & r_{P-1}^* \\ r_1 & r_0 & \ddots & \vdots \\ \vdots & \ddots & \ddots & r_{k_1}^* \\ r_{P-1} & \cdots & r_1 & r_0 \end{bmatrix}_{P \times P}. \quad (5)$$

It is easy to observe that $|r_1|^2, \dots, |r_{P-1}|^2$ can be suppressed by minimizing $\|\tilde{\mathbf{X}}^* \tilde{\mathbf{X}} - N\mathbf{I}\|^2$ (hereafter $\|\cdot\|$ denotes the Frobenius matrix norm). Note that in this case, CAP assumes $w_k = 2(P - k)$ for r_k ($k = 1, \dots, P - 1$) in the WISL metric defined in Eq. (3), and 0 weights for the other correlation lags. In the more general case of suppressing $r_{k_1}, \dots, r_{k_{Q-1}}$, $\tilde{\mathbf{X}}^* \tilde{\mathbf{X}}$ may not be a Toeplitz matrix and a general expression for w_k does not exist. Yet we can still suppress $r_{k_1}, \dots, r_{k_{Q-1}}$ by minimizing the criterion $\|\tilde{\mathbf{X}}^* \tilde{\mathbf{X}} - N\mathbf{I}\|^2$, which is "almost equivalent" to the following optimization problem:

$$\begin{aligned} \min_{\{x_n\}_{n=1}^N, \mathbf{U}} & \left\| \tilde{\mathbf{X}} - \sqrt{N}\mathbf{U} \right\|^2 \\ \text{s.t. } & \mathbf{U}^* \mathbf{U} = \mathbf{I} \text{ and } |x_n| = 1, n = 1, \dots, N \end{aligned} \quad (6)$$

where \mathbf{U} is an $(N + P - 1) \times Q$ semi-unitary matrix.

Eq. (6) can be solved in the following cyclic way. The matrix $\tilde{\mathbf{X}}$ is first set to an initial value. Then Eq. (6) is iteratively minimized by fixing $\{x_n\}_{n=1}^N$ to compute \mathbf{U} , then fixing \mathbf{U} to compute $\{x_n\}_{n=1}^N$ and so on, until a given stop criterion is satisfied. We refer the readers to [14] for details.

3. CAN

It is well-known that

$$\left| \sum_{n=1}^N x_n e^{-j\omega n} \right|^2 = \sum_{k=-(N-1)}^{N-1} r_k e^{-j\omega k} \triangleq \Phi(\omega) \quad (7)$$

for any $\omega \in [0, 2\pi]$ (see, e.g., [15]). Then it is not difficult to prove that the ISL metric in Eq. (2) is proportional to the following frequency-domain metric:

$$\text{ISL} \propto \sum_{p=1}^{2N} [\Phi(\omega_p) - N]^2 = \sum_{p=1}^{2N} \left[\left| \sum_{n=1}^N x_n e^{-j\omega_p n} \right|^2 - N \right]^2,$$

where $\omega_p = 2\pi p/2N$, $p = 1, \dots, 2N$. The above criterion leads to the following minimization problem:

$$\min_{\{x_n\}_{n=1}^N, \{\psi_p\}_{p=1}^{2N}} \sum_{p=1}^{2N} \left| \sum_{n=1}^N x_n e^{-j\omega_p n} - \sqrt{N} e^{j\psi_p} \right|^2. \quad (8)$$

Define a unitary $2N \times 2N$ matrix $\mathbf{A} = \frac{1}{\sqrt{2N}} [\mathbf{a}_1 \cdots \mathbf{a}_{2N}]$ where $\mathbf{a}_p^* = [e^{-j\omega_p} \cdots e^{-j2N\omega_p}]$. Then the criterion in

Eq. (8) can be rewritten as $\|\mathbf{A}^* \mathbf{z} - \mathbf{v}\|^2$ (to within a multiplicative constant), where $\mathbf{z} = [x_1 \cdots x_N \ 0 \cdots 0]^T$ and $\mathbf{v} = \frac{1}{\sqrt{2}} [e^{j\psi_1} \cdots e^{j\psi_{2N}}]^T$. Similarly to CAP, the new criterion $\|\mathbf{A}^* \mathbf{z} - \mathbf{v}\|^2$ can be cyclically minimized by the following algorithm which we call CAN (CA-new):

Step 0: Initialize $\{x_n\}_{n=1}^N$ by a randomly generated or a good existing sequence such as the Golomb sequence [5].
Step 1: Fix $\{x_n\}_{n=1}^N$ and compute $\psi_p = \arg(f_p)$, $p = 1, \dots, 2N$ where $\mathbf{f} = \mathbf{A}^* \mathbf{z}$ denotes the FFT of \mathbf{z} .
Step 2: Fix $\{\psi_p\}_{p=1}^{2N}$ and compute $x_n = e^{j \arg(g_n)}$, $n = 1, \dots, N$ where $\mathbf{g} = \mathbf{A} \mathbf{v}$ denotes the IFFT of \mathbf{v} (note that $\|\mathbf{A}^* \mathbf{z} - \mathbf{v}\|^2 = \|\mathbf{z} - \mathbf{A} \mathbf{v}\|^2$).
Step 3: Repeat Steps 1 and 2 until a pre-specified stop criterion is satisfied (e.g., $\|\mathbf{x}^{(i)} - \mathbf{x}^{(i+1)}\| < 10^{-3}$, where $\mathbf{x}^{(i)}$ is the sequence obtained at the i^{th} iteration).

Because of FFT operations, the CAN algorithm can be used to design sequences up to $N \sim 10^6$ or even larger.

4. WeCAN

WeCAN deals with the WISL metric in a similar way that CAN deals with the ISL metric. It is not difficult to prove that

$$\text{WISL} = \sum_{k=1}^{N-1} \gamma_k^2 |r_k|^2 = \frac{1}{4N} \sum_{p=1}^{2N} [\tilde{\Phi}(\omega_p) - \gamma_0 N]^2, \quad (9)$$

where $\tilde{\Phi}(\omega_p) = \sum_{k=-(N-1)}^{N-1} \gamma_k r_k e^{-j\omega_p k} = \tilde{\mathbf{x}}_p^* (\gamma_0 \mathbf{\Gamma}) \tilde{\mathbf{x}}_p$,

$$\mathbf{\Gamma} = \frac{1}{\gamma_0} \begin{bmatrix} \gamma_0 & \gamma_1 & \cdots & \gamma_{N-1} \\ \gamma_1 & \gamma_0 & \ddots & \vdots \\ \vdots & \ddots & \ddots & \gamma_1 \\ \gamma_{N-1} & \cdots & \gamma_1 & \gamma_0 \end{bmatrix}, \quad (10)$$

$\tilde{\mathbf{x}}_p = [x_1 e^{-j\omega_p} \ x_2 e^{-j2\omega_p} \ \cdots \ x_N e^{-jN\omega_p}]^T$ and $\omega_p = 2\pi p/2N$, $p = 1, \dots, 2N$. The γ_k (real-valued and $\gamma_k = \gamma_{-k}$) above is related to the weight w_k in Eq. (3) as $w_k = \gamma_k^2$, and it is required that γ_0 be chosen sufficiently large to ensure the positive semi-definiteness of $\mathbf{\Gamma}$ (denoted as $\mathbf{\Gamma} \geq 0$).

By substituting $\tilde{\mathbf{x}}_p^* (\gamma_0 \mathbf{\Gamma}) \tilde{\mathbf{x}}_p$ for $\tilde{\Phi}(\omega_p)$ in Eq. (9) we can get $\text{WISL} = \frac{\gamma_0^2}{4N} \sum_{p=1}^{2N} [\tilde{\mathbf{x}}_p^* \mathbf{\Gamma} \tilde{\mathbf{x}}_p - N]^2$, which suggests the following minimization problem

$$\begin{aligned} \min_{\{x_n\}_{n=1}^N, \{\alpha_p\}_{p=1}^{2N}} & \sum_{p=1}^{2N} \|\mathbf{C} \tilde{\mathbf{x}}_p - \alpha_p\|^2 \\ \text{s.t. } & \|\alpha_p\|^2 = N, \quad p = 1, \dots, 2N, \\ & |x_n| = 1, \quad n = 1, \dots, N, \end{aligned} \quad (11)$$

where the matrix \mathbf{C} is a square root of $\mathbf{\Gamma}$, i.e., $\mathbf{\Gamma} = \mathbf{C}^T \mathbf{C}$.

A cyclic algorithm for Eq. (11), which is based on FFT operations and similar to the CAN algorithm in Section 3, can be derived and we call it WeCAN (the details are not shown

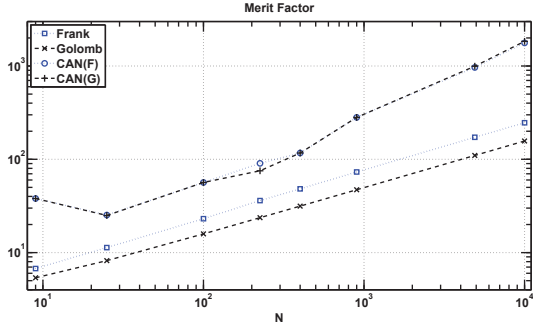


Fig. 1. The merit factors of the Frank, Golomb, CAN(F) and CAN(G) sequences of lengths from 3^2 up to 100^2 .

here due to space limit). Note that, because of the $N \times N$ weighting matrix \mathbf{C} , WeCAN requires N times more FFT operations than CAN. Nonetheless, WeCAN can still be used for relatively large values of N , up to $N \sim 10^4$.

5. NUMERICAL EXAMPLES

5.1. ISL Design

We compare the merit factors of the Golomb sequence ([5]), of the Frank sequence ([9]), and of the CAN sequence initialized by one of these two types of sequences (denoted as CAN(G) and CAN(F), respectively). Because Frank sequences are only defined for lengths that are perfect squares (note that the CAN sequence does not have such a limitation), we let $N = 3^2, 5^2, 10^2, 15^2, 20^2, 30^2, 70^2$ and 100^2 . The results are shown in Figure 1 using a log-log scale. For all sequence lengths we consider, the CAN(G) and CAN(F) sequences give close merit factors; both are much larger than the merit factors given by the Golomb or Frank sequence. When $N = 10^4$, the CAN(G) sequence provides the largest merit factor of 1839.8. Additionally we compute the CAN(G) sequence of length 2^{20} (longer than 10^6), whose MMF is 53076 and is more than thirty times larger than the MMF given by the Golomb sequence of the same length (which is 1608).

5.2. WISL Design - A First Example

Consider the design of a data sequence of length $N = 100$, with the aim of suppressing the correlations r_1, \dots, r_{25} and r_{70}, \dots, r_{79} . The MMF weights in Eq. (3) are correspondingly chosen as: $w_k = 1$ if $k \in [1, 25] \cup [70, 79]$ and $w_k = 0$ otherwise.

We use the WeCAN algorithm in Section 4 to generate the sequence. We choose $\gamma_k = 1$ for $k \in [1, 25] \cup [70, 79]$ and $\gamma_k = 0$ for $k \in [26, 69] \cup [80, 99]$. γ_0 is chosen to be 12.05 so that $\Gamma \geq 0$ in Eq. (10). Figure 2 shows the correlation levels (20 $\log_{10} |r_k/r_0|$) of the so-obtained WeCAN sequence and the CAN(G) sequence of $N = 100$ from the last subsection, together with their MMF values. As expected, the WeCAN sequence shows much lower correlation levels at the required

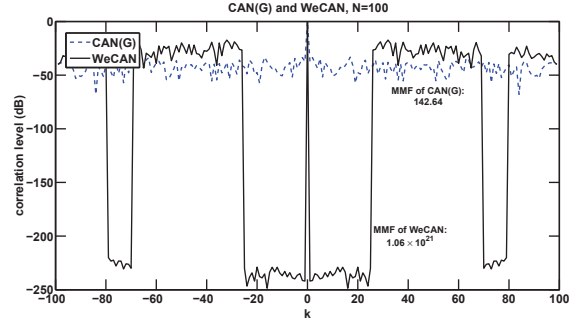


Fig. 2. Correlation levels of the CAN(G) and the WeCAN sequence of length $N = 100$, with the aim of suppressing r_1, \dots, r_{25} and r_{70}, \dots, r_{79} .

time lags and the MMF of the WeCAN sequence is significantly larger than that of the CAN(G) sequence.

5.3. WISL Design - A Second Example

Consider, once again, the design of a data sequence of length $N = 100$ but now with the aim of suppressing the correlations r_1, \dots, r_{39} . In this case the MMF weights in Eq. (3) become $w_k = 1$ if $k \in [1, 39]$ and $w_k = 0$ otherwise. We use the CAP algorithm in Section 2 to generate the sequence. We choose $P = Q = 40$ and thus $\tilde{\mathbf{X}} = \tilde{\mathbf{X}}$ in Eq. (4).

Figure 3 shows the correlation levels of the so-obtained CAP sequence and the CAN(G) sequence of $N = 100$, together with their MMF values. The CAP sequence achieves practically 0 correlation sidelobes from r_1 up to r_{P-1} (-300 dB is close to 10^{-16} , the smallest number that can be properly handled in MATLAB), and the corresponding MMF can be considered to be infinity. It is also worth mentioning that the CAP algorithm is able to provide an infinite MMF in principle only if $N - 1 \geq 2(P - 1)$. The reason is that the number of the degrees of freedom is $N - 1$ (there are $N - 1$ free phases and the initial phase does not matter) and our goal is to match $2(P - 1)$ real numbers (i.e., the real and imaginary parts of r_1, \dots, r_{P-1}). In the next example, $N = 200$ and $P = 40$, in which case the CAP sequence also provides an infinite MMF.

Remark: In the examples in this and the last subsection, we use a randomly generated sequence to initialize CAP or WeCAN. Different initializations lead to different sequences, which however, have similar correlation properties. Another fact worth pointing out is the computational efficiency of the proposed algorithms: each of the above numerical examples (for each N) can be finished in MATLAB in a normal PC within minutes, except the computation of the CAN(G) sequence of length 2^{20} which takes hours.

5.4. FIR Channel Estimation

Consider an FIR channel impulse response $\{h_p\}_{p=0}^{P-1}$ whose estimation is our main goal. Suppose we transmit a probing sequence $\{x_n\}_{n=1}^N$ and obtain the received signal $\mathbf{y} = \tilde{\mathbf{X}}\mathbf{h} + \mathbf{e}$, where $\tilde{\mathbf{X}}$ is as defined in Eq. (4), $\mathbf{y} = [y_1 \ \dots \ y_{N+P-1}]^T$,

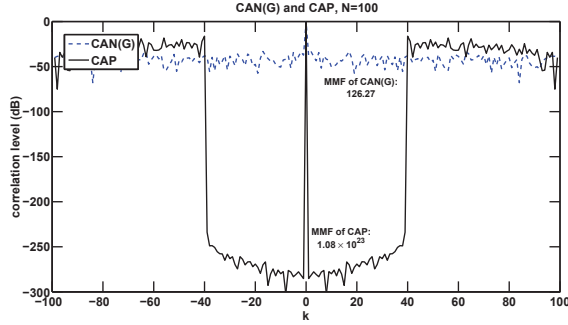


Fig. 3. Correlation levels of the CAN(G) and the CAP sequence of length $N = 100$, with the aim of suppressing r_1, \dots, r_{39} .

$\mathbf{h} = [h_0 \ \dots \ h_{P-1}]^T$ and $\mathbf{e} = [e_1 \ \dots \ e_{N+P-1}]^T$ ($\{e_n\}_{n=1}^{N+P-1}$ is i.i.d. complex Gaussian white noise of zero mean and variance σ^2). We use $\bar{\mathbf{x}}_p$, the p^{th} column of $\bar{\mathbf{X}}$, as a “matched filter” to determine h_p from \mathbf{y} : $\hat{h}_p = \frac{1}{N} \bar{\mathbf{x}}_p^* \mathbf{y}$.

Let $P = 40$ and $\{h_p\}_{p=0}^{P-1}$ is randomly generated (we let both the real and imaginary part of h_p exponentially decrease and then add some random noise). We compare the Golomb sequence and the CAP sequence. N is fixed at 200 and σ^2 is varied from 10^{-6} to 1. For each pair (N, σ^2) , 500 Monte-Carlo trials are run (the noise \mathbf{e} is varied) and the MSE of $\hat{\mathbf{h}}$ is shown in Figure 4. Due to better correlation properties (actually 0 sidelobes from r_1 to r_{P-1}), the CAP sequence generates consistently smaller MSE than the Golomb sequence. In particular, the MSE of $\hat{\mathbf{h}}$ corresponding to the CAP sequence will become 0 if σ^2 goes to 0, while the performance of the Golomb sequence is limited to a certain level because of its non-zero correlation sidelobes.

6. CONCLUDING REMARKS

We have presented several cyclic algorithms, namely CAP, CAN and WeCAN which can be used to design unimodular sequences that have good autocorrelation properties. CAN can be used to design very long sequences (of length N up to 10^6), which can hardly be handled by other algorithms proposed in the previous literature. CAN deals with the ISL metric whereas CAP and WeCAN aim to minimize weighted-ISL metrics. We have shown that, in particular, CAP and WeCAN can be used to design sequences that have virtually zero autocorrelation sidelobes in a specified lag interval. CAP and WeCAN can be used for $N \sim 10^3$ or larger, depending on how many lags are considered. A number of numerical examples have been provided to demonstrate the good autocorrelation properties of the unimodular sequences designed using the proposed algorithms.

7. REFERENCES

[1] J. Jedwab, “A survey of the merit factor problem for binary sequences,” *Sequences and Their Applications - SETA 2004*, vol. 3486, pp. 30–55, Springer Berlin / Heidelberg, 2005.

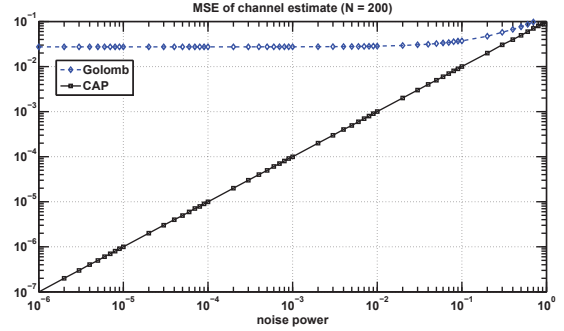


Fig. 4. The MSE of the estimated $\hat{\mathbf{h}}$ using the Golomb sequence and the CAP sequence.

[2] R. Ferguson and J. Knauer, “Optimization methods for binary sequences - the merit factor problem,” *MITACS 6th Annual Conference*, University of Calgary, Alberta, Canada, May 2005.

[3] H. Schotten and H. Lücke, “On the search for low correlated binary sequences,” *International Journal of Electronics and Communications*, vol. 59, no. 2, pp. 67–78, 2005.

[4] P. Rapajic and R. Kennedy, “Merit factor based comparison of new polyphase sequences,” *IEEE Communications Letters*, vol. 2, no. 10, pp. 269–270, October 1998.

[5] N. Zhang and S. Golomb, “Polyphase sequence with low autocorrelations,” *IEEE Transactions on Information Theory*, vol. 39, no. 3, pp. 1085–1089, May 1993.

[6] A. Brenner, “Polyphase barker sequences up to length 45 with small alphabets,” *Electronics Letters*, vol. 34, no. 16, pp. 1576–1577, Aug 1998.

[7] P. Borwein and R. Ferguson, “Polyphase sequences with low autocorrelation,” *IEEE Transactions on Information Theory*, vol. 51, no. 4, pp. 1564–1567, April 2005.

[8] U. Somaini and M. Ackroyd, “Uniform complex codes with low autocorrelation sidelobes (corresp.),” *IEEE Transactions on Information Theory*, vol. 20, no. 5, pp. 689–691, September 1974.

[9] R. Frank, “Polyphase codes with good nonperiodic correlation properties,” *IEEE Transactions on Information Theory*, vol. 9, no. 1, pp. 43–45, January 1963.

[10] F. Kretschmer Jr. and K. Gerlach, “Low sidelobe radar waveforms derived from orthogonal matrices,” *IEEE Transactions on Aerospace and Electronic Systems*, vol. 27, no. 1, pp. 92–102, January 1991.

[11] H. Khan, Y. Zhang, C. Ji, C. Stevens, D. Edwards, and D. O’Brien, “Optimizing polyphase sequences for orthogonal netted radar,” *IEEE Signal Processing Letters*, vol. 13, no. 10, pp. 589–592, October 2006.

[12] P. Stoica, J. Li, and X. Zhu, “Waveform synthesis for diversity-based transmit beam pattern design,” *IEEE Transactions on Signal Processing*, vol. 56, no. 6, pp. 2593–2598, June 2008.

[13] J. Tropp, I. Dhillon, R. Heath, and T. Strohmer, “Designing structured tight frames via an alternating projection method,” *IEEE Transactions on Information Theory*, vol. 51, no. 1, pp. 188–209, January 2005.

[14] J. Li, P. Stoica, and X. Zheng, “Signal synthesis and receiver design for MIMO radar imaging,” *IEEE Transactions on Signal Processing*, vol. 56, no. 8, pp. 3959–3968, August 2008.

[15] P. Stoica and R. Moses, *Spectral Analysis of Signals*, Prentice Hall, Upper Saddle River, NJ, 2005.